

**Positron or Positroniumlike Surface State on Al(100)?**

K. G. Lynn

*Brookhaven National Laboratory, Upton, New York 11973*

and

A. P. Mills, Jr.

*AT&T Bell Laboratories, Murray Hill, New Jersey 07974*

and

R. N. West

*University of East Anglia, Norwich, NR4 7TJ, England*

and

S. Berko and K. F. Canter

*Brandeis University, Waltham, Massachusetts 02154*

and

L. O. Roellig

*City College of the City University of New York, New York, New York 10031*

(Received 28 December 1984)

Using a high-intensity beam of 200-eV positrons we have measured the two-dimensional angular correlation of the  $2\gamma$  annihilation radiation from a clean Al(100) surface. The momentum distribution identified with the positron surface state has a nearly isotropic conical shape and a  $(7.1 \pm 0.5)$ -mrad full width at half maximum. The data are not consistent with a simple interpretation based on either the usual model of a positron bound in a surface state by its "image-correlation potential" or a positronium atom weakly bound to the surface.

PACS numbers: 71.60.+z, 73.20.-r, 71.25.Hc

Positron annihilation offers a unique way to observe the momentum distribution of electrons in solids.<sup>1</sup> The positron is not a weakly interacting probe and significantly increases the density of electrons in its vicinity.<sup>2</sup> Thus the positron annihilation rate in a metal is much greater than the independent-particle-model prediction. Nevertheless, theory and experiment have shown that the momentum distributions obtained from the angular correlation of the  $2\gamma$  annihilation radiation (ACAR) can yield valuable information about electron wave functions, and faithfully reflect the Fermi surface of metals and alloys. It is interesting to ask if an analogous picture will hold for positrons localized at the surface of a metal.

The extension of the ACAR technique to the study of surfaces requires positrons with energy low enough to stop near a sample surface. It is well established that a large fraction of the positrons implanted into a single-crystal metal at a few hundred electronvolts of kinetic energy diffuse back to the surface and become trapped in a surface state.<sup>3</sup> The positrons in this surface state annihilate with near-surface electrons and thus can give new information about these electrons. Beams of slow positrons with sufficient intensity for practical surface ACAR measurements are now available.<sup>4</sup> The usefulness of such measurements will

depend greatly on the nature of the positron surface state and how well we understand it. While there are many model calculations, we are presently lacking a firm theoretical foundation.

Early ACAR results obtained on the internal surfaces of voids in metals<sup>5</sup> motivated the development of theories describing the positron interaction with surfaces. The most frequently used model has been that of a positron tightly bound to a surface in its image-correlation potential well.<sup>6,7</sup> A second model is that of a positronium (Ps) atom weakly bound to the surface by Van der Waals forces.<sup>8</sup> It is not clear in either case that ACAR measurements will be uncontaminated by effects due to the momentum of the positron state. In order to find out more about the positron surface state we have made ACAR measurements on a simple *s-p* metal surface, Al(100). Our measurements show that neither picture is completely accurate.

The apparatus for this experiment consists of a high-intensity reactor-produced <sup>64</sup>Cu positron source, an ultrahigh-vacuum (UHV) target chamber, and a pair of Anger cameras with associated electronics.<sup>9</sup> The high-purity Cu sources were irradiated as 3-mm-diam spheres for 48 h at  $8 \times 10^{14} n^0 \text{ cm}^{-2} \text{ sec}^{-1}$ . The resulting 80-Ci sources were introduced into the UHV source chamber through an air lock by remote control.

The  $^{64}\text{Cu}$  was evaporated *in situ* onto a W(110) substrate prepared by heating to form a self-moderating source of  $\approx 10^7$  slow positrons per sec.

The slow positrons were guided by an axial magnetic field and accelerated onto the Al target. Unwanted counts from  $^3\text{S}_1$  Ps and from positrons that might miss the target were eliminated by shielding made of 90% W alloy around the target and by Pb shielding outside the vacuum system. The 99.999%-pure Al(100) single-crystal sample was  $\text{Ar}^+$ -ion bombarded and annealed at  $\approx 550^\circ\text{C}$  before each run. We observed a sharp (100) low-energy electron diffraction pattern and found the surface to be contaminated by  $< 1\%$  of a monolayer of O and C by Auger spectroscopy before each run. The  $2\gamma$  annihilation photons were detected in coincidence by two Anger cameras located 6.3 m on either side of the sample. The combined 9.5-mm full width at half maximum (FWHM) resolution of the pair of detectors thus corresponds to an angular resolution of 1.5 mrad. The (100) Al sample surface was parallel to a line connecting the centers of the Anger cameras and a [100] direction in the surface plane was oriented  $20^\circ$  from this line.

We obtained spectra using 200-eV and 15-keV positrons. At these two incident positron energies we know that  $\approx 98\%$  and  $\approx 7\%$  of the positrons diffuse back to the surface.<sup>3</sup> We also obtained a bulk Al spectrum using an Al- $^{22}\text{Na}$ -Al sandwich located within 0.5 mm of the Al(100) sample position. This spectrum is in agreement with the 15-keV spectrum except that the latter has a 30% very broad component typical of a transition metal. Examination of our positron beam spot after the data were taken showed that it is reasonable to assign this component to positrons that hit the stainless-steel heater stage. Since this component is much broader than our surface two-dimensional (2D) ACAR data to be presented below, its contribution is only about 5% of the peak height at  $p=0$ . At our present level of precision this essentially flat contribution can be ignored.

Our 2D ACAR data obtained with 200-eV positrons is shown in Fig. 1. This set of data has been smoothed with a two-channel (1.2-mrad) FWHM Gaussian. The one-sided contribution due to the annihilation of fast singlet Ps is immediately evident. The fast Ps<sup>10</sup> is moving in the direction away from the surface,  $p_\perp > 0$ . (Note that the positive axis is on the left-hand side of the figures.) Figure 2(a) shows contours of the same data, unsmoothed and corrected only for the momentum sampling function by use of the measured single-camera response function. We fold these data about  $p_\perp = 0$  and subtract the  $p_\perp < 0$  half from the  $p_\perp > 0$  half to determine the shape and amplitude of the fast-Ps component.<sup>11</sup> To compensate in first order for the unphysical sharp cutoff introduced by this subtraction procedure, the difference distribution is then convo-

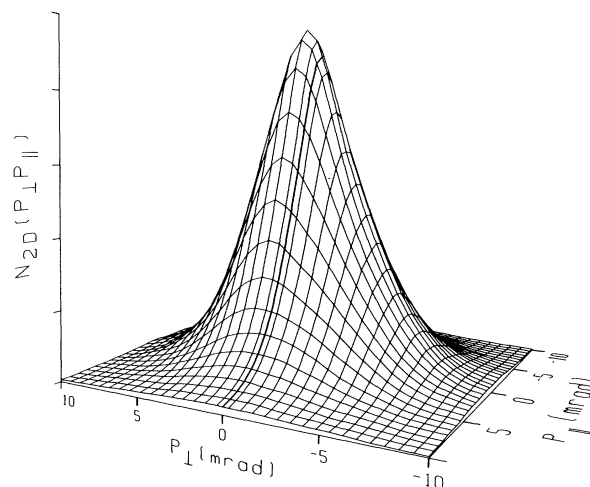


FIG. 1. Two-dimensional angular-correlation spectra for 200-eV positrons incident upon a clean Al(100) surface. Note that the positive axis is on the left-hand side of the curve. The total number of counts is  $3 \times 10^5$ .

luted with the detector resolution. We thus obtain our best estimate for the fast-Ps component as shown in Fig. 2(b) and it is in rough agreement with the time-of-flight measurements.<sup>12</sup> The total amount of fast singlet Ps is  $16\% \pm 2\%$  and agrees with what we expect on the basis of the known fast-Ps total yield<sup>3</sup> of 50% to 60% of the fraction of the positrons that hit the Al(100) sample.<sup>13</sup> The amount of fast Ps obtained by analyzing the 15-keV data in the same manner is  $1\% \pm 1\%$ . We subtract the fast-Ps component from the original data of Fig. 2(a) to obtain the surface 2D ACAR-momentum contours in Fig. 2(c). Except for the Ps component, these contours represent unsmoothed data.

The distribution in Fig. 2(c) has a conical shape that is very similar to the distribution that has been observed by 2D ACAR on Al containing voids.<sup>14</sup> Contrary to our expectations based on the simple surface-state models,<sup>6-8</sup> this distribution is nearly isotropic. To expose the shape with better statistics, we present in Fig. 3 projections (1D integrals) of the momentum distribution along  $p_\perp$  and  $p_\parallel$ , i.e., we produce one-dimensional ACAR curves. The FWHM are  $7.1 \pm 0.5$  mrad for both projections.<sup>15</sup> The model of a bound positron in its "image-correlation-potential" well<sup>7</sup> produces a strong anisotropy which is essentially independent of the details of the model potential. The picture of a weakly bound Ps atom<sup>8</sup> where the parallel motion would be thermal and the perpendicular motion would be that associated with the 0.5-eV Ps binding energy also predicts anisotropy. Furthermore, the latter model would result in a distribution that is narrower than our angular resolution in both direc-

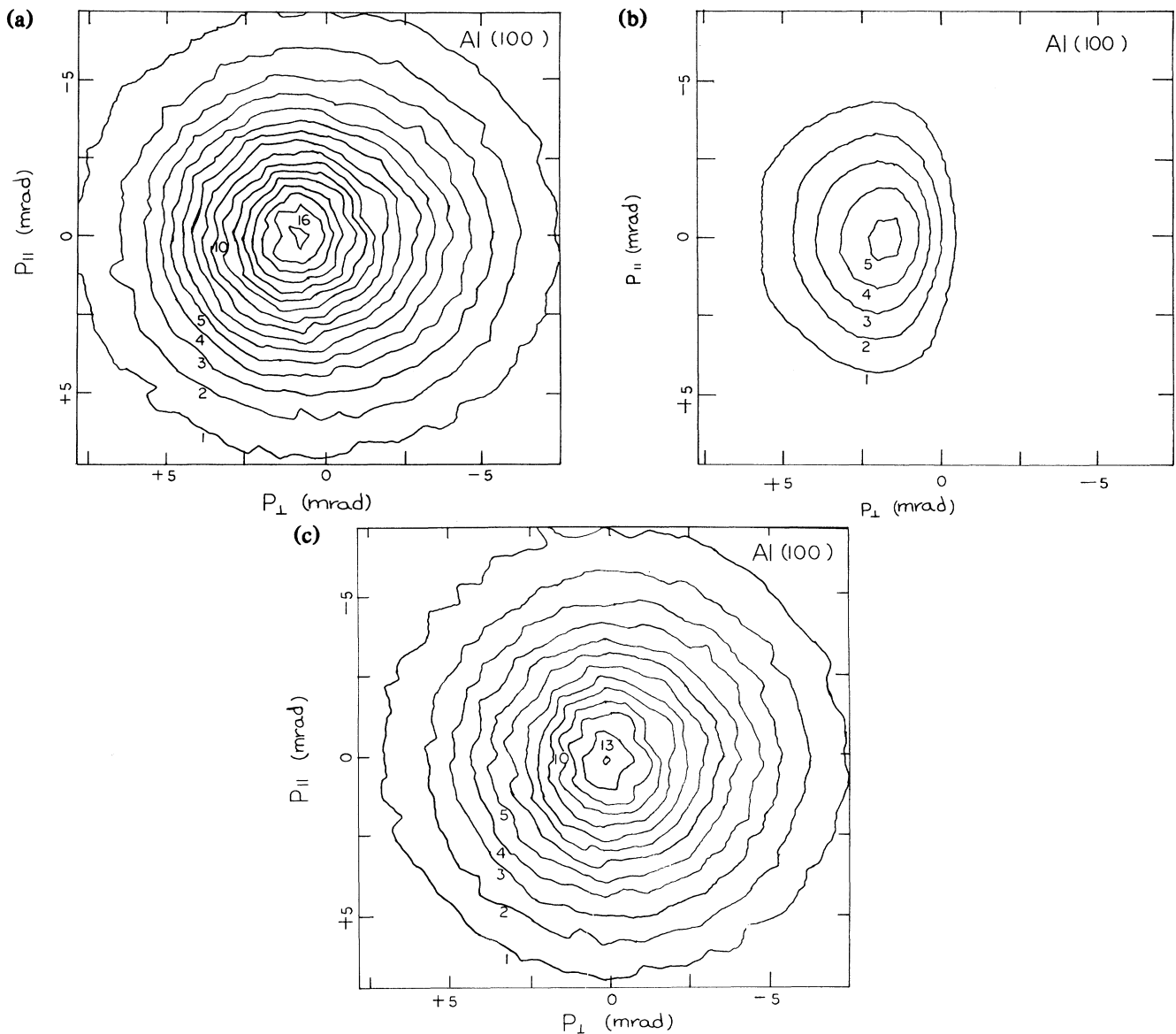


FIG. 2. (a) Data of Fig. 1 presented as an unsmoothed 2D ACAR contour plot. (b) Fast-Ps contours obtained from the difference between the  $p_{\perp} > 0$  and  $p_{\perp} < 0$  halves of (a). The data have been smoothed by a Gaussian of similar width (2 channels) to that of the resolution to remove the unphysically sharp cutoff at  $p = 0$ . (c) 2D ACAR contours for the positron surface state obtained by subtracting the fast-Ps component (b) from the original data (a).

tions. Both of these models are inconsistent with our data. We note, however, that some lack of a large anisotropy could be explained if we were to assume that the positron state is not extended in the direction parallel to the surface but is localized at some surface defect, or by impurity atoms.

We conclude that neither surface-state model predicts correctly the angular distribution of the annihilation photons. It is obvious that the positronium picture needs to be supplemented by inclusion of the

effects of electron exchange, and that the positron picture lacks an accurate description of correlation effects. It is hoped that our experiment will be an impetus for the development of an improved model of the positron surface state.

We are grateful to M. McKeown and R. Lee for assistance with the data analysis, M. Weber, J. Rutherford, and D. M. Chen for help in the experiment, W. Frieze and G. Plain for help in the initial stages of this work, and high-flux beam reactor operations staff

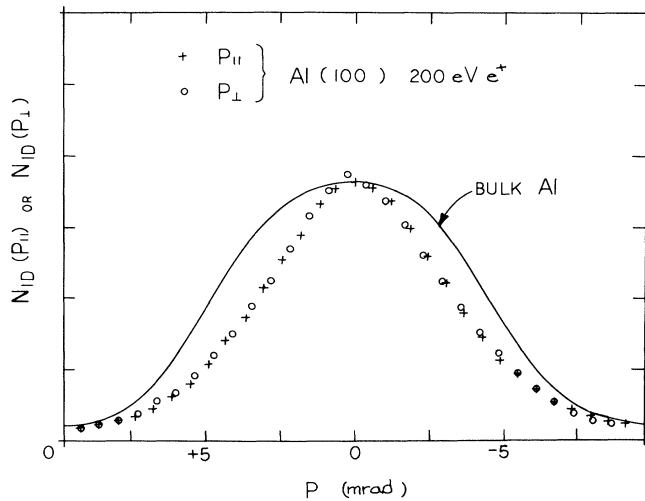


FIG. 3. One-dimensional projections of the surface positron ACAR spectrum for momentum parallel and perpendicular to the surface. For comparison we also show the spectrum obtained for positrons annihilating in bulk Al. The three spectra have been normalized to equal peak heights.

for producing the  $\text{Cu}^{64}$  pellets. We would also like to thank P. M. Platzman for many enlightening discussions. This work was supported in part by the Division of Materials Sciences, U. S. Department of Energy, under Contract No. DE-AC02-76CH00016, and in part by the National Science Foundation through Grant No. DMR-8315691.

*Note added.*—We have now repeated our measurements using a clean Al(110) sample. The surface ACAR momentum distribution is again nearly isotropic but has a slightly wider full width at half maximum ( $8.0 \pm 0.5$  mrad) than our Al(100) data presented in this Letter.

<sup>1</sup>See, for example, S. Berko, in *Positron Solid State Physics*,

edited by W. Brandt and A. Dupasquier (North-Holland, New York, 1983), p. 64, and references therein.

<sup>2</sup>See, for example, J. P. Carbotte, in Ref. 1, p. 32, and references therein.

<sup>3</sup>See, for example, K. G. Lynn, in Ref. 1, p. 609; A. P. Mills, Jr., in Ref. 1, p. 432, and references therein.

<sup>4</sup>In addition to the intense positron beam at Brookhaven, there are linac-based pulsed positron beams in operation. See, for example, R. H. Howell, R. A. Alvarez, and M. Stanek, *Appl. Phys. Lett.* **40**, 751 (1982). Howell *et al.* have recently obtained 2D-surface ACAR data on a Cu sample [R. Howell, P. Meyer, I. J. Rosenberg, and M. J. Fluss, preceding Letter [*Phys. Rev. Lett.* **54**, 1698 (1985)]]].

<sup>5</sup>O. Mogensen, K. Petersen, R. M. J. Cotterill, and B. Hudson, *Nature (London)* **239**, 98 (1972); R. M. J. Cotterill, I. K. MacKenzie, L. Smedskjaer, G. Trumpy, and J. H. O. L. Traff, *Nature (London)* **239**, 99 (1972).

<sup>6</sup>C. H. Hodges and M. J. Stott, *Solid State Commun.* **12**, 1153 (1973).

<sup>7</sup>R. Nieminen and M. Manninen, *Solid State Commun.* **15**, 403 (1974).

<sup>8</sup>P. M. Platzman and N. Tzoar, to be published.

<sup>9</sup>R. N. West, J. Mayers, and P. A. Walters, *J. Phys. E* **14**, 478 (1981).

<sup>10</sup>A. Isii, *Surf. Sci.* **147**, 295 (1984).

<sup>11</sup>The  $p_{\perp}=0$  positron is found to within  $\pm 0.1$  mrad by minimizing of the mean square difference between the left- and right-hand halves of the bulk-Al data; the  $p_{\perp}=0$  point so determined was the same for the 15-keV data.

<sup>12</sup>A. P. Mills, Jr., L. Pfeiffer, and P. M. Platzman, *Phys. Rev. Lett.* **51**, 1085 (1983).

<sup>13</sup>Our estimate of singlet fast-Ps yield varies depending on the choice of the  $p_{\perp}$  point. Changing this point by  $\pm 0.3$  mrad from the optimum point (see Ref. 11 above) changes the fast-Ps component by  $\pm 6.5\%$ . The agreement between our measurement of the Ps yield and the known value from earlier experiments (see Ref. 3) thus confirms that our determination of  $p_{\perp}=0$  is correct to within  $\pm 0.15$  mrad.

<sup>14</sup>W. Triftshauser, J. D. McGervey, and R. W. Hendricks, *Phys. Rev. B* **9**, 3321 (1974); A. Alam, P. A. Walters, R. N. West, and J. D. McGervey, *J. Phys. F* **14**, 761 (1984).

<sup>15</sup>The  $\pm 0.5$ -mrad error bar is our estimate of the systematic uncertainty associated with our uncertainty in the  $p_{\perp}=0$  position (see Ref. 13). Varying the  $p_{\perp}=0$  position by  $\pm 0.15$  mrad leads to at most a 10% anisotropy with the parallel being larger.